

A genetic pathway composed of Sox14 and Mical governs severing of dendrites during pruning

Daniel Kirilly^{1,7}, Ying Gu^{1,2,7}, Yafen Huang¹, Zhuohao Wu³, Arash Bashirullah⁴, Boon Chuan Low², Alex L Kolodkin³, Hongyan Wang^{5,6} & Fengwei Yu^{1,2,5}

Pruning that selectively eliminates neuronal processes is crucial for the refinement of neural circuits during development. In *Drosophila*, the class IV dendritic arborization neuron (ddaC) undergoes pruning to remove its larval dendrites during metamorphosis. We identified Sox14 as a transcription factor that was necessary and sufficient to mediate dendrite severing during pruning in response to ecdysone signaling. We found that Sox14 mediated dendrite pruning by directly regulating the expression of the target gene *mical*. *mical* encodes a large cytosolic protein with multiple domains that are known to associate with cytoskeletal components. *mical* mutants had marked severing defects during dendrite pruning that were similar to those of *sox14* mutants. Overexpression of Mical could significantly rescue pruning defects in *sox14* mutants, suggesting that Mical is a major downstream target of Sox14 during pruning. Thus, our findings indicate that a previously unknown pathway composed of Sox14 and its cytoskeletal target Mical governs dendrite severing.

The selective removal of exuberant or inaccurate neuronal processes without causing neuronal death, referred to as pruning, is crucial for the refinement of neural circuits in the developing nervous system^{1,2}. Pruning shares several features with neuronal degeneration in response to injury or disease¹. In injured neurons, axons distal to the lesion site rapidly degenerate, a process known as Wallerian degeneration^{1,3–5}. In neurodegenerative disorders, breakage and degeneration of neuronal processes derived from the diseased neurons often occur before neuronal death^{6,7}. In *Drosophila*, larval-born neurons undergo extensive remodeling or apoptosis to form the adult nervous system during metamorphosis⁸. The remodeled neurons survive, but prune their neuronal processes/connections before eclosion, which later regrow to become part of the adult nervous system⁸. These pruning events occur primarily in the first 24 h of metamorphosis in the CNS and peripheral nervous systems (PNS)^{9–11}. In the CNS, the mushroom body γ neurons, olfactory projection neurons and thoracic ventral neurons remodel their larval dendrites/axons to form adult connectivities^{5,9–18}. In the PNS, the majority of larval neurons, including class II and III dendritic arborization sensory neurons, are eliminated via apoptosis. However, certain class I and IV dendritic arborization neurons survive to undergo large-scale dendrite-specific pruning with minimal morphological changes in their axon termini^{19,20}.

The class IV dendritic arborization neuron ddaC undergoes a stereotyped pruning process that is initiated by the severing of proximal dendrites, followed by rapid fragmentation of severed dendrites and clearance of cellular debris via phagocytosis. During dendrite pruning, severing events consistently occur at the proximal regions

of dendrites. Initial signs of dendrite severing include blebbing and proximal thinning of dendrites, involving the depolymerization of microtubule and actin cytoskeletons^{19,21}. The steroid molting hormone 20-hydroxyecdysone (ecdysone), a master regulator that controls body-plan changes in insects, regulates both these pruning events in neurons undergoing remodeling and apoptosis of select PNS neurons during metamorphosis^{19,20}. The ubiquitin-proteasome system and Dronc caspase act to execute the pruning process, along with Ik2 kinase and the microtubule-severing factor Katanin-60L1 (refs. 21–23). How ecdysone regulates a transcriptional hierarchy to mediate dendrite pruning, however, is unknown.

We found that Sox14 serves as an important regulator of dendrite severing in ddaC neurons. We found that Sox14, a critical target of ecdysone signaling, was both necessary and sufficient to induce dendrite severing during pruning. Sox14 mediates dendrite severing by promoting the expression of a direct target, *mical*, which was also required for dendrite severing. The Mical protein consists of multiple domains that are known to interact with actin and other cytoskeletal proteins and potentially mediates cytoskeletal alterations during dendrite pruning. Thus, our findings reveal a genetic pathway composed of the transcription factor Sox14 and its downstream target Mical that mediates dendrite severing in class IV ddaC neurons in response to ecdysone.

RESULTS

The class I and IV dendritic arborization neurons in the PNS survive and undergo a stereotyped pruning process in each abdominal hemisegment

¹Temasek Life Sciences Laboratory and the ²Department of Biological Sciences, National University of Singapore, Singapore. ³Solomon H. Snyder Department of Neuroscience, Howard Hughes Medical Institute, The Johns Hopkins School of Medicine, Baltimore, Maryland, USA. ⁴Division of Pharmaceutical Sciences, University of Wisconsin, Madison, Wisconsin, USA. ⁵Neuroscience and Behavioral Disorder Program, Duke–National University of Singapore Graduate Medical School Singapore, Singapore. ⁶Department of Physiology, Yong Loo Lin School of Medicine, National University of Singapore, Singapore. ⁷These authors contributed equally to this work. Correspondence should be addressed to F.Y. (fengwei@tll.org.sg).

Received 30 June; accepted 4 September; published online 1 November 2009; doi:10.1038/nn.2415

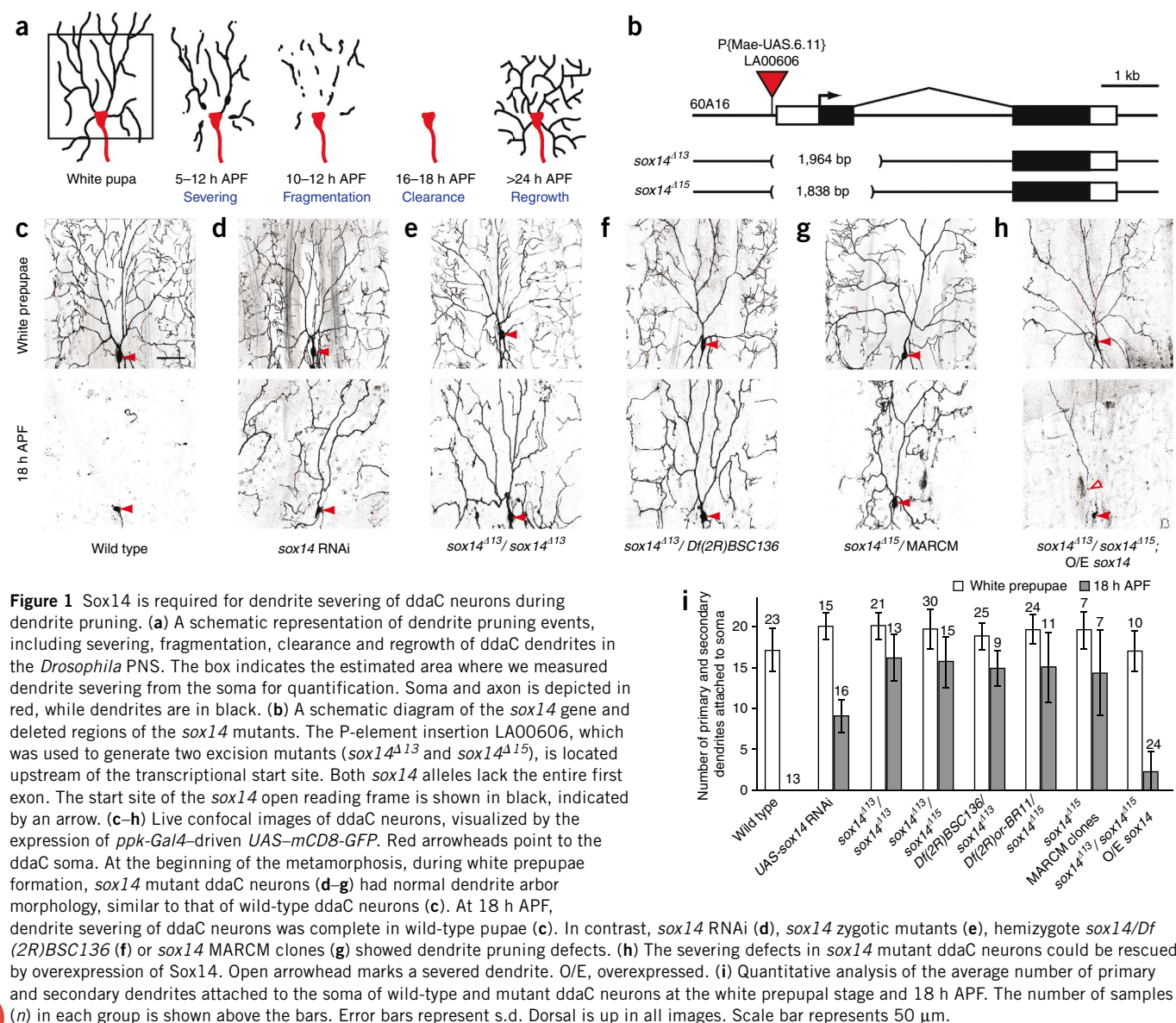


Figure 1 Sox14 is required for dendrite severing of ddaC neurons during dendrite pruning. **(a)** A schematic representation of dendrite pruning events, including severing, fragmentation, clearance and regrowth of ddaC dendrites in the *Drosophila* PNS. The box indicates the estimated area where we measured dendrite severing from the soma for quantification. Soma and axon is depicted in red, while dendrites are in black. **(b)** A schematic diagram of the *sox14* gene and deleted regions of the *sox14* mutants. The P-element insertion LA00606, which was used to generate two excision mutants (*sox14*^{Δ113} and *sox14*^{Δ115}), is located upstream of the transcriptional start site. Both *sox14* alleles lack the entire first exon. The start site of the *sox14* open reading frame is shown in black, indicated by an arrow. **(c–h)** Live confocal images of ddaC neurons, visualized by the expression of *ppk-Gal4*-driven *UAS-mCD8-GFP*. Red arrowheads point to the ddaC soma. At the beginning of the metamorphosis, during white prepupae formation, *sox14* mutant ddaC neurons **(d–g)** had normal dendrite arbor morphology, similar to that of wild-type ddaC neurons **(c)**. At 18 h APF, dendrite severing of ddaC neurons was complete in wild-type pupae **(c)**. In contrast, *sox14* RNAi **(d)**, *sox14* zygotic mutants **(e)**, hemizygote *sox14*/Df(2R)BSC136 **(f)** or *sox14* MARCM clones **(g)** showed dendrite pruning defects. **(h)** The severing defects in *sox14* mutant ddaC neurons could be rescued by overexpression of Sox14. Open arrowhead marks a severed dendrite. O/E, overexpressed. **(i)** Quantitative analysis of the average number of primary and secondary dendrites attached to the soma of wild-type and mutant ddaC neurons at the white prepupal stage and 18 h APF. The number of samples (*n*) in each group is shown above the bars. Error bars represent s.d. Dorsal is up in all images. Scale bar represents 50 μm.

during the early phase of metamorphosis^{19,20}. We focused our attention on the class IV ddaC neuron that is located in the dorsal cluster and can be labeled by the expression of membrane-bound mCD8–green fluorescent protein (GFP) using the class IV–specific *pickpocket* (*ppk*)-*Gal4* driver (*ppk-Gal4*) (Fig. 1)²⁴. ddaC neurons started to show signs of dendritic instability at approximately 5 h after puparium formation (5 h APF), when small blebs formed along the proximal branches of dendrites (Fig. 1a and Supplementary Movie 1). These blebs migrated dynamically along the dendrites, resulting in thinning and subsequent physical breakage of the dendrites from the soma (Supplementary Movie 1), namely dendrite severing. The severing of proximal dendrites was apparent at 8 h APF and completed by 12 h APF (Fig. 1a, Supplementary Fig. 1 and Supplementary Movie 1). Over the next 6 h, severed dendrites underwent rapid fragmentation and clearance by phagocytes (Fig. 1a and Supplementary Fig. 1). At 18 h APF, no larval dendrites were observed in the vicinity of the ddaC soma, whereas the soma and the axon remained intact (Fig. 1a and Supplementary Fig. 1). Any defects in dendrite-severing events can be easily recognized by the presence of dendrites that remain attached to the soma at 18 h APF.

The transcription factor Sox14 mediates dendrite severing

Ecdysone is an important regulator of neuronal remodeling events in mushroom body γ neurons of the CNS¹¹ and dendritic arborization neurons of the PNS^{19,20}. Ecdysone binds to a nuclear receptor heterodimer consisting of ecdysone receptor and Ultraspiracle (EcR/Usp), resulting in the activation of target gene expression during *Drosophila* metamorphosis²⁵. The B1 isoform of the ecdysone receptor (EcR-B1) is highly expressed in remodeling neurons of the CNS^{11,18} and the PNS²⁰. EcR-B1 expression is activated by TGF-β signaling and the cohesin complex during the larval-pupal transition^{26–28}. Inactivation of EcR/Usp functions that blocks ecdysone signaling not only inhibits neuronal pruning in both systems, but also prevents cell death in apoptotic dendritic arborization neurons^{11,19,20}. To identify previously unknown proteins that mediate dendrite pruning downstream of EcR/Usp, we carried out an RNA interference (RNAi) screen and tested genes that, from previous microarray analyses, have the potential to respond to ecdysone signaling^{29–31}. We isolated *sox14*, which, when attenuated by RNAi, resulted in severe dendrite pruning defects in all ddaC neurons. *sox14* RNAi

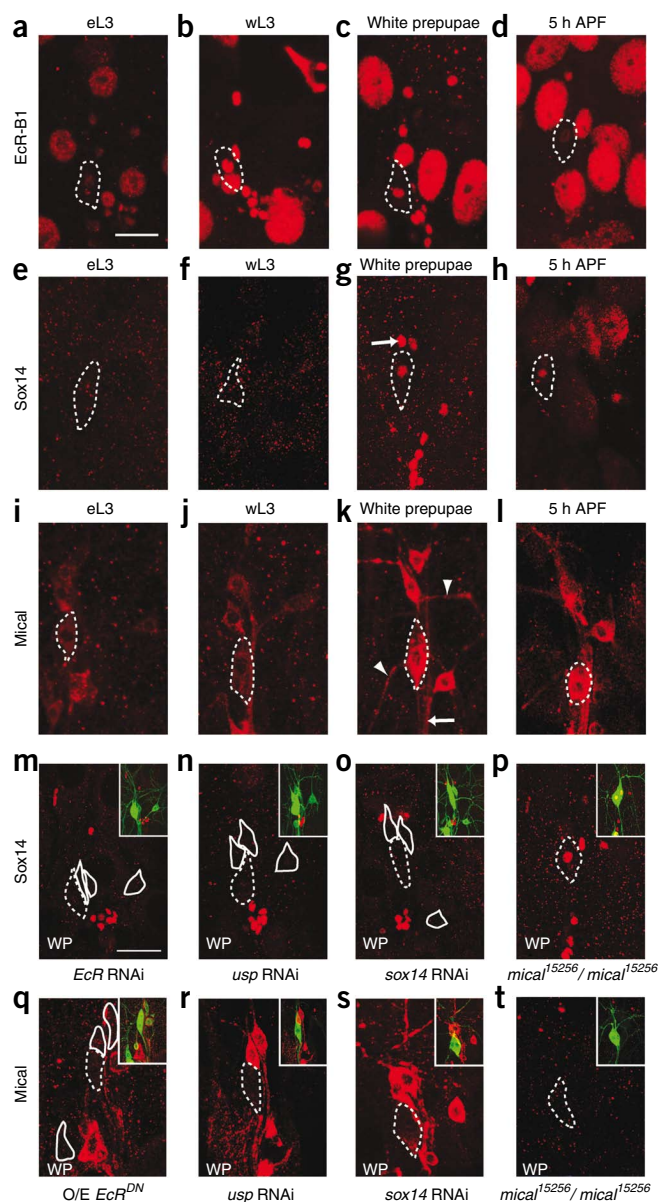


Figure 2 Mical localization is dependent on Sox14 and EcR/Usp in ddaC neurons. (a–l) Expression of EcR-B1, Sox14 and Mical at the eL3, wL3, white prepupal and 5 h APF stages. ddaC neurons are marked by dashed lines. Their location was determined by *ppk-Gal4*-driven mCD8-GFP expression. The expression of EcR-B1 (a–d), Sox14 (e–h) and Mical (i–l) in ddaC neurons were compared at various stages. Mical was concentrated in the soma, but it was also present in the dendrites (arrowheads) and axons (arrow) (k). For each individual antibody, immunofluorescence staining at various time points was processed in the same tube and images were taken at the same gain. (m–t) Sox14 and Mical immunostaining in various mutants. Neurons overexpressing RNAi or dominant-negative constructs were labeled by the expression of mCD8-GFP (green) driven by the *Gal4*¹⁰⁹⁽²⁾⁸⁰ (m–o, q) or *ppk-Gal4* driver (r, s). Insets show the expression of the transgenes, indicated by GFP. ddaC neurons are marked by dashed lines and other dendritic arborization neurons are shown by solid lines. Sox14 expression was regulated by ecdysone signaling (m–p). Sox14 expression was abolished in all of the dendritic arborization neurons when ecdysone signaling was blocked by *EcR* RNAi or *usp* RNAi (m, n). Sox14 can also be effectively downregulated in all *sox14* RNAi dendritic arborization neurons (o). However, Sox14 expression was unaffected in *mical*¹⁵²⁵⁶ mutant (p). (q–t) Mical expression was dependent on the ecdysone receptor complex and Sox14. Mical expression was strongly reduced in *EcR*^{DN} (q), *usp* RNAi (r) or *sox14* RNAi (s) ddaC neurons and was absent from *mical*¹⁵²⁵⁶ mutant (t). WP, white prepupae. Scale bar represents 20 μm.

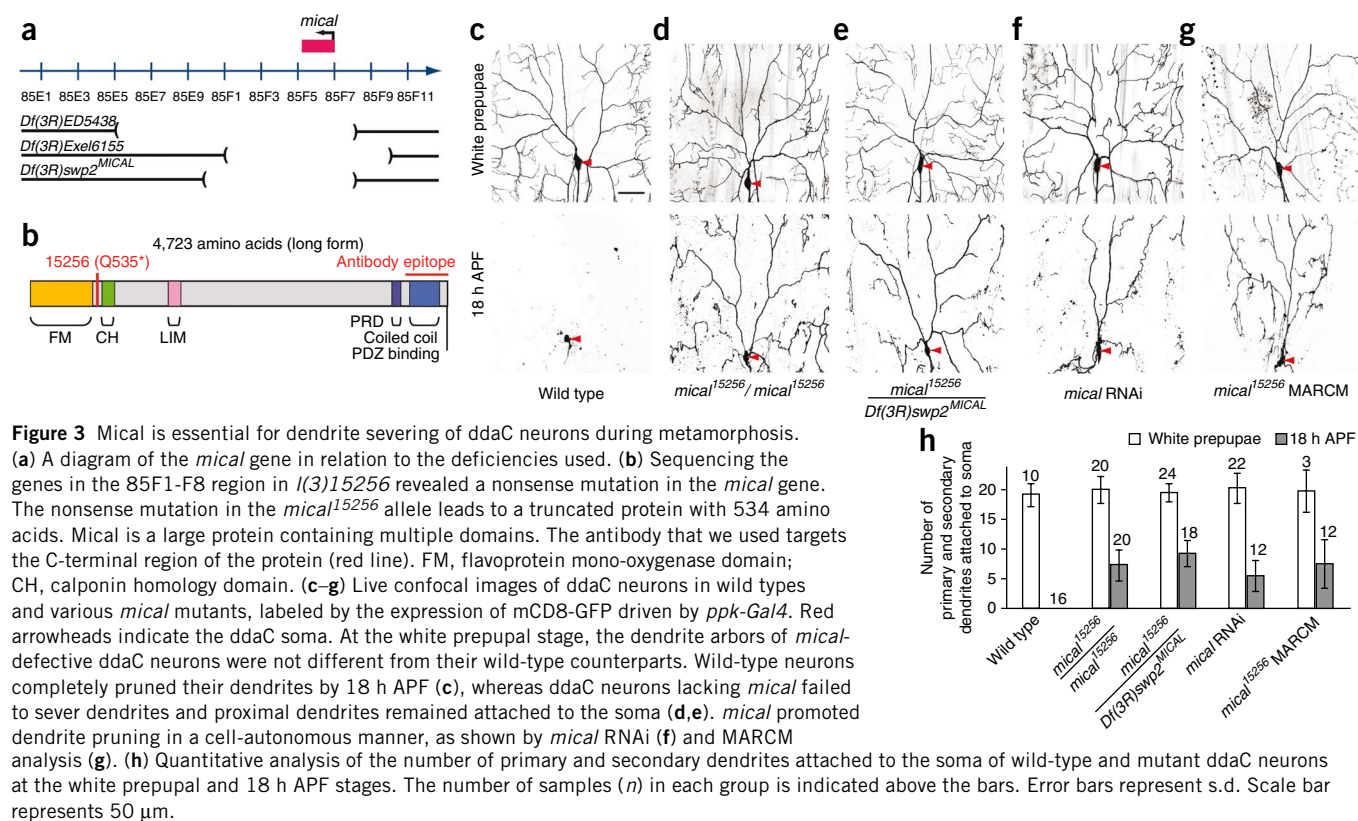
pruning defects in the early pupal stage. The defects in dendrite severing that we observed in both of the *sox14* homozygous mutants were more pronounced than those induced by *sox14* RNAi at 18 h APF. In these *sox14* mutants, the majority of the primary and secondary dendrites remained attached to the ddaC soma at 18 h APF (100%, $n = 13$; **Fig. 1e,i** and **Supplementary Movie 2**) and 24 h APF (**Supplementary Fig. 1**), compared with those present in the white prepupae (**Fig. 1e**). Transheterozygotes between *sox14*^{Δ13} and *sox14*^{Δ15}, or hemizygotes between *sox14*^{Δ13} or *sox14*^{Δ15} and either of the small deficiencies removing the *sox14* gene, showed indistinguishable dendrite-severing defects compared to either of the homozygotes (**Fig. 1f,i**). In addition, we were unable to detect Sox14 protein via immunofluorescence analysis in *sox14*^{Δ13} (**Supplementary Fig. 3**) or *sox14*^{Δ15} mutants (data not shown). Thus, both *sox14*^{Δ13} and *sox14*^{Δ15} are either strong hypomorphic or null alleles, and we refer to them as *sox14* mutants. Using the mosaic analysis with a repressible cell marker (MARCM) technique³², we generated homozygous clones for *sox14* mutants. The same *sox14* ddaC clones were first examined in white prepupae and subsequently at 18 h APF for potential pruning defects (**Fig. 1g**). All of the *sox14* ddaC clones had a strong pruning defect at 18 h APF (100%, $n = 7$; **Fig. 1g,i**), suggesting that Sox14 mediates dendrite pruning in a cell-autonomous fashion. Reintroduction of Sox14 into *sox14* mutant ddaC neurons largely rescued dendrite-severing defects ($n = 24$; **Fig. 1h,i**), further confirming that the dendrite pruning defects associated with *sox14* mutants are a result of the loss of *sox14* function.

Wild-type dorsal dendritic arborization neurons such as ddaA, ddaB and ddaF were eliminated via apoptosis at the early pupal stage (**Supplementary Fig. 4**). Knockdown of *sox14* by RNAi using the dendritic arborization neuron driver *Gal4*¹⁰⁹⁽²⁾⁸⁰ inhibited neuronal death in the majority of ddaF (86%, $n = 15$), ddaA and ddaB neurons at 18 h APF (**Supplementary Fig. 4**). Therefore, loss of *sox14* function causes *EcR*-like phenotypes with regard to dendrite pruning and neuronal apoptosis during early metamorphosis.

sox14 transcripts are ubiquitously expressed during embryogenesis and are enriched in the third instar larvae and early pupae^{33,34}. We generated a specific antibody to Sox14 (see Online Methods) and used it to examine Sox14 expression in dendritic arborization neurons, comparing it with EcR-B1 expression (**Fig. 2**). EcR-B1 expression

did not affect the overall morphology of dendritic arbors ($n = 15$; **Fig. 1d** and **Supplementary Fig. 2**), as compared to the wild-type arbor ($n = 23$; **Fig. 1c** and **Supplementary Fig. 2**). Notably, at 18 h APF, approximately nine primary and secondary dendrites were still attached to the soma (100%, $n = 16$; **Fig. 1d,i**), whereas no dendrites were observed in the wild-type ddaC neurons (100%, $n = 13$; **Fig. 1c,i**), suggesting that the severing of proximal dendrites from ddaC neurons requires Sox14. Sox14 is a high-mobility group (HMG)-box transcription factor, the sole *Drosophila* Sox C group protein and belongs to the evolutionarily conserved Sox family. None of the other seven Sox family genes in *Drosophila* appears to be involved in dendrite pruning, as knockdown of these genes by RNAi did not induce an obvious pruning defect in ddaC neurons (data not shown).

To further verify the role of *sox14* in ddaC dendrite pruning, we generated *sox14* mutants by mobilizing a P element, P{Mae-UAS.6.11}LA00606, inserted upstream of the *sox14* gene (**Fig. 1b**). We recovered two excisions, *sox14*^{Δ13} and *sox14*^{Δ15}, in which the entire first exon was removed (**Fig. 1b**). The homozygous *sox14* mutant flies survived until the late pupal stages, allowing us to observe dendrite



was low in ddaC neurons at the early third-instar larval (eL3) stage, reached its peak at the wandering third-instar larval (wL3) and white prepupal stages and declined at 5 h APF (Fig. 2a–d; also seen in a previous study²⁰). In contrast, Sox14 expression was undetectable at the eL3 and wL3 stages, but increased markedly at the white prepupal stage, followed by a slight decrease after the white prepupal stage (Fig. 2e–h). The intensity of Sox14 staining in the nuclei of ddaC neurons was slightly weaker than in those of the apoptotic ddaF neurons (Fig. 2g). Thus, Sox14 is expressed in both apoptotic and remodeling dendritic arborization neurons in white prepupae and prepupae, lagging slightly behind the upregulation of EcR-B1 expression.

Mical, a cytosolic protein, promotes dendrite severing

To search for possible downstream targets of Sox14 involved in dendrite pruning, we screened a collection of ethyl-methyl-sulfonate mutagenized late-pupal lethal mutations on the third chromosome (Fig. 3)³⁵. We isolated a mutant, *l(3)15256*, that showed a failure of dendrite severing in ddaC neurons by 18 h APF (Fig. 3d, Supplementary Fig. 1 and Supplementary Movie 3). *l(3)15256* ddaC neurons retained an average of 7.4 primary and secondary dendrites attached to the soma at 18 h APF (100%, *n* = 20; Fig. 3d,h) and 3 dendrites at 24 h APF (100%, *n* = 13; Supplementary Fig. 1), indicating that the mutant neurons had a strong severing defect. The overall larval dendrite morphology of ddaC neurons in the wL3 larvae of *l(3)15256* zygotic mutant was indistinguishable from that of wild-type ddaC neurons, as judged by the number of terminal dendrites (Supplementary Fig. 2). The *l(3)15256* mutation was mapped to the cytological region 85F1-F8 (Fig. 3a) and further sequence analysis in this region identified a nonsense mutation in the *mical* gene that predicted the production of a truncated protein with only the first 534 amino acids (Fig. 3b). Mical is a large, cytosolic, multidomain

protein containing a flavoprotein mono-oxygenase domain at the N terminus, a calponin homology domain and LIM domain at the middle region, and a proline-rich domain (PRD), coiled-coil domain and PDZ-binding motif at the C terminus (Fig. 3b)³⁶. The Mical protein was undetectable in *l(3)15256* homozygous white prepupae (Fig. 2t), as compared with wild type (Fig. 2k). Hemizygotes of *l(3)15256* with a small deficiency, *Df(3R)swp2*^{MICAL}, that removes the *mical* gene³⁶ or four other previously identified *mical* mutants³⁷ also caused equally strong dendrite-severing defects (Fig. 3e,h and Supplementary Fig. 5). Therefore, *l(3)15256* is probably a null allele of *mical* and we refer to it as *mical*¹⁵²⁵⁶. Moreover, the dendrite-pruning defects associated with *mical* mutants can be fully rescued by overexpressing full-length Mical (Mical^{FL}), but not by expressing an N-terminal portion of Mical (Mical^{N-ter}) in ddaC neurons (Supplementary Fig. 6). These results suggest that the dendrite-pruning defects observed in *mical*¹⁵²⁵⁶ mutant neurons are attributable to a loss of *mical* function. Thus, *mical* is important in dendrite severing of ddaC neurons. *mical* RNAi (100%, *n* = 12; Fig. 3f,h) and *mical*¹⁵²⁵⁶ MARCM clones (100%, *n* = 12; Fig. 3g,h) also showed a severing defect in ddaC neurons, similar to *mical* zygotic mutants. These data establish a cell-autonomous role for *mical* during dendrite pruning.

Moreover, similar to observations in *EcR*^{DN} (*EcR-B1-W650A*) or *sox14* mutants, *mical* dendritic arborization neurons ddaD and ddaE failed to prune their dendritic processes by 24 h APF (Supplementary Fig. 7). Surprisingly, unlike pruning defects observed in *sox14* mutants, apoptotic neurons such as ddaF neurons were eliminated at 18 h APF in *mical* zygotic mutants (Supplementary Fig. 4), *mical* MARCM clones or *mical* RNAi (data not shown). Thus, Mical is specifically required for dendrite severing of class I and IV dendritic arborization neurons, but is dispensable for neuronal apoptosis in other apoptotic dendritic arborization neurons during early metamorphosis.

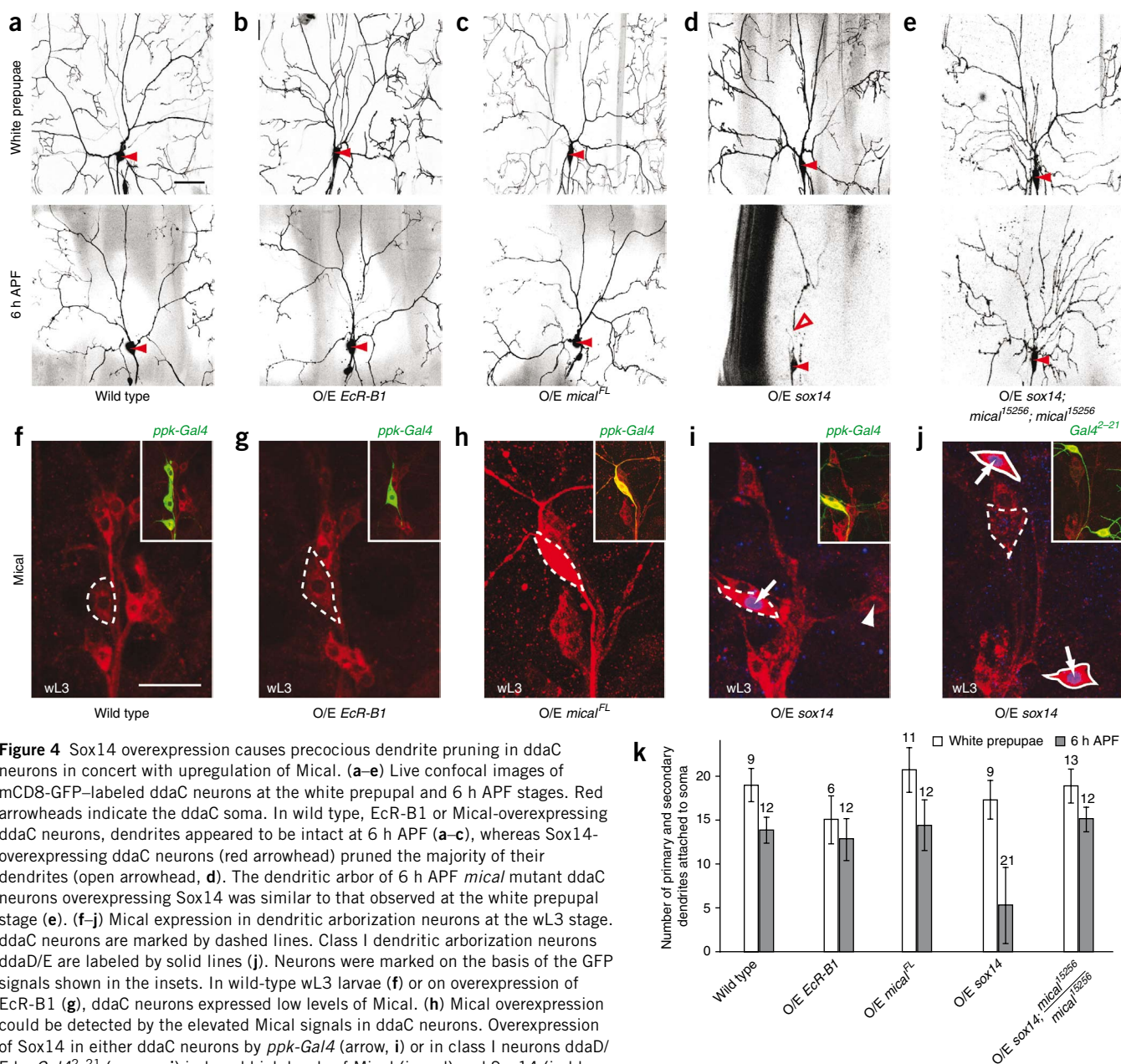


Figure 4 Sox14 overexpression causes precocious dendrite pruning in ddaC neurons in concert with upregulation of Mical. (**a–e**) Live confocal images of mCD8-GFP-labeled ddaC neurons at the white prepupal and 6 h APF stages. Red arrowheads indicate the ddaC soma. In wild type, EcR-B1 or Mical-overexpressing ddaC neurons, dendrites appeared to be intact at 6 h APF (**a–c**), whereas Sox14-overexpressing ddaC neurons (red arrowhead) pruned the majority of their dendrites (open arrowhead, **d**). The dendritic arbor of 6 h APF *mical* mutant ddaC neurons overexpressing Sox14 was similar to that observed at the white prepupal stage (**e**). (**f–j**) Mical expression in dendritic arborization neurons at the wL3 stage. ddaC neurons are marked by dashed lines. Class I dendritic arborization neurons ddaD/E are labeled by solid lines (**j**). Neurons were marked on the basis of the GFP signals shown in the insets. In wild-type wL3 larvae (**f**) or on overexpression of EcR-B1 (**g**), ddaC neurons expressed low levels of Mical. (**h**) Mical overexpression could be detected by the elevated Mical signals in ddaC neurons. Overexpression of Sox14 in either ddaC neurons by *ppk-Gal4* (arrow, **i**) or in class I neurons ddaD/E by *Gal4²⁻²¹* (arrows, **j**) induced high levels of Mical (in red) and Sox14 (in blue, arrows) expression. An arrowhead indicates a ddaE neuron in **i**. (**k**) Quantification of the number of primary and secondary dendrites attached to the soma of various genotypes at the white prepupal and 6 h APF stages. The number of samples (*n*) in each group is indicated above the bars. Error bars represent s.d. Scale bars represent 50 and 20 μ m in **a** and **f**, respectively.

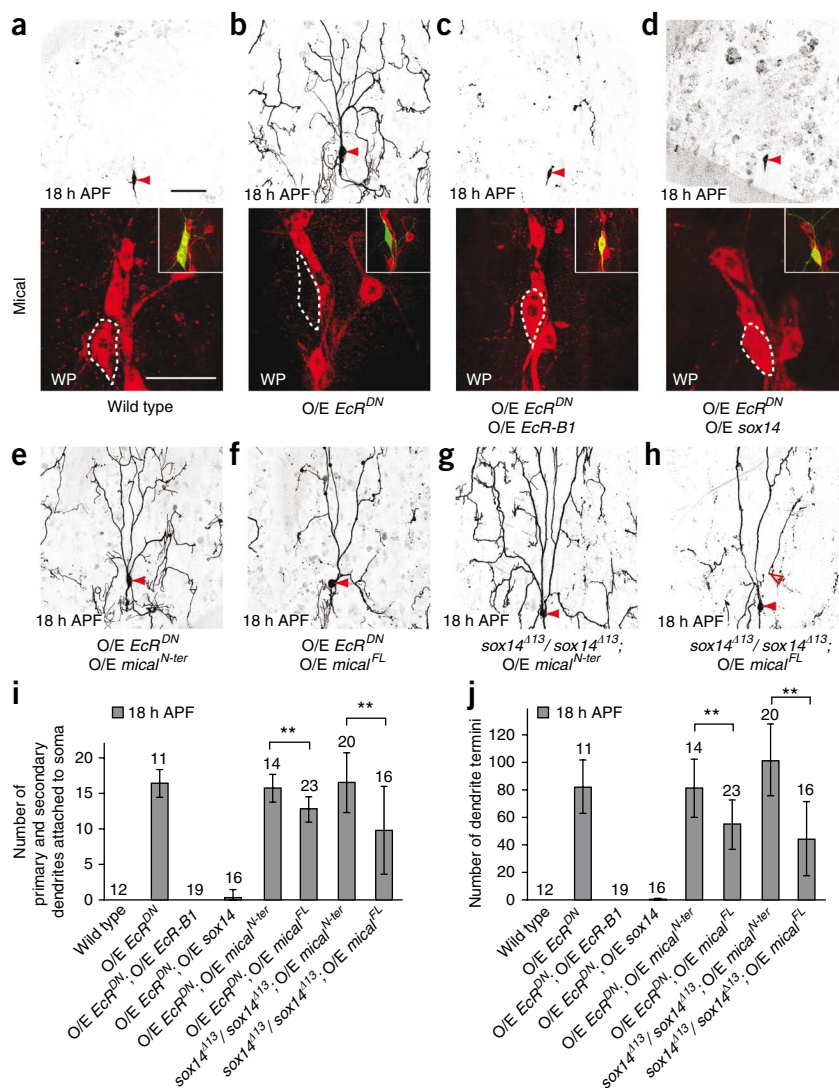
Upregulation of Mical requires *EcR*, *usp* and *sox14*

We next determined the expression pattern of Mical and its requirement with respect to *EcR*, *usp* and *sox14* using a previously characterized antibody to Mical³⁶. We further verified the specificity of this antibody, as it did not stain *mical* mutants (**Fig. 2t**) or *mical* RNAi-treated ddaC neurons (data not shown), but staining with it did lead to markedly enhanced signals when Mical was overexpressed in *mical* mutant ddaC neurons (**Supplementary Fig. 6**). Mical was expressed at low levels in the eL3 and wL3 larvae (**Fig. 2i,j**). However, we observed substantially elevated Mical expression at the white prepupal and 5 h APF stages in all of the dendritic arborization neurons (**Fig. 2k,l**). In dendritic arborization

neurons, Mical was localized in both dendrites (arrowheads) and axons (arrow), and in the cytoplasm in soma (**Fig. 2k**).

Upregulation of Mical protein temporally coincided with Sox14 expression (**Fig. 2e–l**) and lagged slightly behind the EcR-B1 upregulation (**Fig. 2a–d**). To ascertain whether Sox14 and Mical are downstream targets of EcR-B1 during dendrite pruning, we first examined whether Sox14 and Mical expression is affected in ddaC neurons when ecdysone signaling is blocked. *EcR* RNAi effectively downregulated EcR-B1 expression (**Supplementary Fig. 8**), as compared with wild type (**Supplementary Fig. 8**), and caused strong ddaC pruning defects at 18 h APF (data not shown) that were similar to those in *usp* RNAi-treated or *EcR^{DN}* ddaC neurons (**Supplementary Fig. 1**). We

Figure 5 Mical acts downstream of EcR-B1 and Sox14 during severing. (**a–d**) Top panels, Sox14 overexpression suppressed *EcR^{DN}* pruning defects. Wild-type ddaC neurons pruned their dendrites by 18 h APF (**a**), whereas severing of dendrites was inhibited by overexpression of *EcR^{DN}* (**b**). The pruning defect caused by *EcR^{DN}* was rescued by coexpressing either wild-type EcR-B1 (**c**) or Sox14 (**d**). Bottom panels, Mical immunostaining at the white prepupal stage in various genotypes. High-level expression of Mical in wild type (**a**) at the white prepupal stage could be eliminated in *EcR^{DN}* ddaC neurons (**b**). Mical expression was restored on coexpression of wild-type EcR-B1 (**c**) or Sox14 (**d**) in the *EcR^{DN}* ddaC neurons. ddaC neurons are marked by dashed lines on the basis of the GFP signals shown in the insets. WP, white prepupae. (**e–h**) Mical functioned downstream of EcR-B1 and Sox14 during dendrite pruning. Mical^{FL} (**f**), but not the nonfunctional Mical^{N-ter} (**e**), ameliorated the pruning defect resulting from *EcR^{DN}* overexpression. Overexpression of Mical^{FL} (**h**) significantly rescued ($P < 0.001$) the pruning defect of *sox14* mutant ddaC neurons compared with the controls overexpressing Mical^{N-ter} (**g**). Red arrowheads indicate ddaC soma. (**i–j**) Quantification of the number of primary and secondary dendrites attached to the soma (**i**) and the number of dendrite termini of attached dendrites (**j**) of wild-type and mutant ddaC neurons during metamorphosis. In **i** and **j**, the number of samples (n) in each group is indicated above each bar and error bars represent s.d. ** $P < 0.001$. Scale bars represent 50 μ m (**a**, top panel) and 20 μ m (**a**, bottom panel).



used these strains to block ecdysone signaling in all of the dendritic arborization neurons (using the *Gal4¹⁰⁹⁽²⁾⁸⁰* driver) or in only ddaC neurons (using the *ppk-Gal4* driver) and analyzed Sox14 and Mical expression in mutant dendritic arborization neurons at the white prepupal stage. The inhibition of ecdysone signaling by *EcR* RNAi ($n = 13$; **Fig. 2m**), *EcR^{DN}* (data not shown) or *usp* RNAi ($n = 11$; **Fig. 2n**) resulted in the depletion of Sox14 proteins in all of the dendritic arborization neurons. Likewise, Mical expression failed to increase at the white prepupal stage in *EcR^{DN}* (100%, $n = 18$; **Fig. 2q**) and *usp* RNAi-treated (100%, $n = 17$; **Fig. 2r**) dendritic arborization neurons, in contrast with wild-type white prepupae (**Fig. 2k**). We then examined whether Sox14 is required for Mical expression in ddaC neurons. Mical expression was no longer upregulated in *sox14* RNAi-treated (100%, $n = 14$; **Fig. 2s**) or *sox14* mutant ddaC neurons (100%, $n = 20$; data not shown). On the other hand, EcR-B1 expression appeared to be normal in both *sox14* ($n = 6$; **Supplementary Fig. 8**) and *mical* mutants ($n = 9$; **Supplementary Fig. 8**), and Sox14 levels in *mical* mutants remained the same as those in wild type ($n = 11$ mutants and 25 wild types; **Fig. 2g,p**). Taken together, Mical and Sox14 are downstream targets of EcR/Usf and Mical upregulation requires Sox14 in ddaC neurons during early metamorphosis.

The temporal regulation of EcR-B1, Sox14 and Mical protein expression in mushroom body γ neurons was highly similar to that observed in dendritic arborization sensory neurons (**Supplementary Fig. 9**). High levels of *sox14* and *mical* transcripts could be detected in mushroom body γ neurons at the white prepupal stage in an

EcR-dependent fashion (**Supplementary Fig. 10**). Notably, *sox14* RNAi caused downregulation of *mical* RNA in mushroom body γ neurons (**Supplementary Fig. 10**). Sox14 was able to directly bind to the *mical* regulatory regions in ecdysone-treated S2 cells (**Supplementary Figs. 10 and 11**). Furthermore, *sox14* RNAi-treated mutants exhibited severe axon-pruning defects in mushroom body γ neurons, whereas the axon branches were pruned normally in homozygous *mical* mutant by 24 h APF (**Supplementary Fig. 10**).

Sox14 overexpression causes precocious severing

Given that *sox14* and *mical* are required for dendrite pruning in ddaC neurons, we next examined whether overexpression of either one is sufficient to cause precocious pruning (**Fig. 4**). At 6 h APF, the majority of primary and secondary dendrites were still attached to the soma in wild-type ddaC neurons (**Fig. 4a**), although the overall dendritic morphology was simple, presumably as a result of the gradual retraction of high-order dendrites. We therefore chose this time point for the detection of potential precocious dendrite severing when EcR-B1, Sox14 or Mical were overexpressed in ddaC neurons. Sox14, when overexpressed in ddaC neurons, substantially accelerated the progression of dendrite pruning, including severing and debris clearance (**Fig. 4d**). By 6 h APF, fewer than five primary and secondary dendrites remained attached to the soma in Sox14-overexpressing ddaC neurons

(Fig. 4d,k), compared with approximately 14 attached dendrites in the wild-type ddaC neurons (Fig. 4a,k). Notably, almost half of the ddaC neurons retained three or fewer attached dendrites, whereas elimination of the majority of disconnected dendritic arbors was observed (40%, $n = 20$; Fig. 4d). Although overexpression of Sox14 reduced the density of high-order dendrites, it did not obviously affect the number of primary and secondary dendrites in white prepupal ddaC neurons (Fig. 4a,d). Thus, Sox14 is an important transcription factor that is necessary and sufficient to promote dendrite severing in ddaC neurons. Continuous overexpression of Sox14 from the late embryonic stages to the early pupal stages using the *ppk-Gal4* driver did not cause neuronal apoptosis, as ddaC neurons were still present by 24 h APF (data not shown).

Does Sox14 overexpression cause upregulation of Mical expression? In wild-type wL3 larvae, Mical was expressed at low levels in dendritic arborization neurons (Fig. 4f). Notably, overexpression of Sox14 led to a marked upregulation of Mical levels in more than half of the ddaC neurons (53% $n = 32$; Fig. 4i), as compared with neighboring dendritic arborization neurons lacking Sox14 overexpression (Fig. 4i). Elevated levels of Mical were also observed in Sox14-overexpressing ddaD/E neurons (42%, $n = 12$; Fig. 4j). We then removed the *mical* gene in Sox14-overexpressing ddaC neurons to examine whether loss of Mical suppresses Sox14-mediated precocious dendrite pruning. Notably, removal of *mical* in Sox14-overexpressing ddaC neurons resulted in retention of larval dendritic arbors; approximately 15 primary and secondary dendrites were still attached to the soma at 6 h APF (100%, $n = 12$; Fig. 4e,k) and some persisted until 18 h APF (data not shown). Overexpressing Sox14 in *mical* ddaC neurons also led to a morphological defect in dendritic arbors (Fig. 4e). Thus, precocious dendrite pruning induced by Sox14 overexpression requires Mical function.

Overexpression of EcR-B1 had no effect on the normal progression of severing events (Fig. 4b). It was unable to induce the expression of Sox14 (data not shown) and Mical in the wL3 larvae (100%, $n = 12$; Fig. 4f,g), suggesting that EcR-B1 is not a rate-limiting factor during dendrite pruning of ddaC neurons. Overexpression of Mical did not promote precocious pruning in ddaC neurons (Fig. 4c), suggesting that Mical is an important, but not exclusive, downstream target of Sox14. Therefore, Mical is necessary, but not sufficient, to initiate the severing events during pruning.

Mical acts downstream of EcR-B1 and Sox14 during severing

To further explore whether Sox14 and Mical mediate dendrite pruning in response to ecdysone signaling, we examined whether overexpression of Sox14 or Mical can rescue the pruning defects caused by blocking ecdysone signaling (Fig. 5). Overexpression of EcR^{DN} caused strong dendrite-pruning defects in ddaC neurons and reduced Mical protein expression (100%, $n = 11$; Fig. 5a,b). We first confirmed that the dendrite-pruning defects associated with EcR^{DN} were a result of the inhibition of EcR function. Coexpression of wild-type EcR-B1 and EcR^{DN} in ddaC neurons fully rescued pruning defects in ddaC neurons (100%, $n = 19$; Fig. 5c,i,j) and restored Mical (100%, $n = 21$; Fig. 5c) and Sox14 expression (100%, $n = 14$; data not shown). We then tested whether *sox14* genetically interacts with *EcR-B1* during dendrite pruning. Sox14 overexpression almost fully rescued the pruning defects at 18 h APF in EcR^{DN}-expressing ddaC neurons (94%, $n = 16$; Fig. 5d,i,j). Moreover, Mical expression was also fully restored when Sox14 was overexpressed in EcR^{DN} ddaC neurons (100%, $n = 15$; Fig. 5d). Thus, *sox14* is an important target of ecdysone signaling during pruning; Sox14, after activation by EcR-B1, initiates the expression of its downstream targets, including Mical, and promotes dendrite pruning.

To investigate whether overexpression of Mical could rescue the pruning defects in EcR^{DN} and *sox14* mutant ddaC neurons, we overexpressed Mical^{FL} or nonfunctional Mical^{N-ter} protein in EcR^{DN} or *sox14* mutant ddaC neurons. Notably, overexpression of Mical^{FL} resulted in a partial, but significant, rescue of the pruning defects in EcR^{DN} ddaC neurons ($P < 0.001$), as around 13 primary and secondary dendrites were attached to the soma and 55 terminal branches remained at 18 h APF ($n = 23$; Fig. 5f,i,j). In contrast, when a truncated version of Mical protein lacking the C-terminal PRD, coiled-coil and PDZ-binding domains was overexpressed in EcR^{DN} ddaC neurons, 16 primary and secondary dendrites remained attached to the soma and 82 terminal branches persisted at 18 h APF ($n = 14$; Fig. 5e,i,j), similar to those observed in EcR^{DN} ddaC neurons ($n = 11$; Fig. 5b,i,j). Overexpression of Mical^{FL} led to even more significant rescue of dendrite pruning defects in *sox14* mutant ddaC neurons ($P < 0.001$), as approximately 10 primary and secondary dendrites remained intact and 45 termini remained at 18 h APF ($n = 16$; Fig. 5h,i,j). In contrast, overexpression of nonfunctional Mical^{N-ter} in *sox14* mutants retained around 16 primary and secondary attached dendrites and 100 terminal branches, and failed to rescue dendrite pruning ($n = 20$; Fig. 5g,i,j). Our data suggest a genetic hierarchy composed of *EcR*, *sox14* and *mical* that governs dendrite severing during early metamorphosis (Supplementary Fig. 12).

DISCUSSION

Here, we identified critical functions of Sox14 and its immediate target Mical in severing dendrites of dendritic arborization neurons during early metamorphosis. The proximal regions of dendrites remained attached to the soma and severing failed to occur when Sox14 or Mical was depleted. Consistent with these observations, the expression of both Sox14 and Mical were upregulated during early metamorphosis. Notably, overexpression of Sox14 was able to induce Mical expression and rescue dendrite pruning in EcR^{DN} ddaC neurons, overriding the requirement for EcR-B1. Mical promotes dendrite pruning through its potential association with the cytoskeleton and regulation of cytoskeletal alterations (Supplementary Fig. 12).

Sox14 mediates both dendrite pruning and apoptosis of dendritic arborization sensory neurons in the PNS. Dendrite pruning involving cellular fragmentation and phagocyte-dependent clearance shares features with apoptosis^{19,23}. *sox14* was recently reported to function as a potential pro-death gene and as being involved in the destruction of the midgut and salivary glands³⁸. We found that Sox14 could also regulate apoptosis in certain dendritic arborization neurons. Loss of *sox14* function inhibited apoptosis of ddaF neurons. In apoptotic ddaF neurons, Sox14 expression was often higher than that of remodeling ddaC neurons (Fig. 2g). It is possible that Sox14 functions in a dose-dependent manner to regulate both apoptosis and remodeling of dendritic arborization sensory neurons in the PNS. Supporting this idea, the pro-death gene *reaper* and the caspase gene *dronc*, which are involved in apoptosis and remodeling, were identified as potential targets of Sox14 (ref. 38). Consistently, overexpression of Sox14 is sufficient to induce cell death in cultured *l(2)mbn* cells³⁸. Continuous overexpression of Sox14 in ddaC neurons did not cause neuronal apoptosis. It is likely that the pro-death effect of Sox14 may be effectively antagonized by protective machinery activated in ddaC neurons, such as upregulation of *Drosophila* inhibitor of apoptosis protein 1 (ref. 22).

Sox group genes are known for their roles in regulating major developmental processes by activating gene transcription³⁹. Our results provide several lines of evidence supporting the view that Mical is a downstream target of Sox14. First, similar to Sox14, Mical also

promotes dendrite severing in ddaC neurons. Second, Mical expression is dependent on Sox14 function, as *Mical* mRNA and protein are undetectable or strongly reduced in *sox14* mutants. On the other hand, overexpression of Sox14 was sufficient to induce Mical expression in dendritic arborization neurons at a much earlier time point. Third, we found several potential binding sites for Sox14 in the regulatory region of the *Mical* gene. We also found that Sox14 specifically associated with some of these sites in a chromatin immunoprecipitation assay. Fourth, overexpression of Mical can significantly suppress the dendrite pruning defects in *sox14* mutants. Fifth, the removal of Mical can largely suppress precocious dendrite pruning induced by Sox14 overexpression in ddaC neurons.

How does Mical promote dendrite severing in ddaC neurons? Mical may regulate cytoskeletal alterations or rearrangements of ddaC dendrites via at least two possible mechanisms. Mical can potentially cross-link actin filaments into bundles and networks through its calponin homology domain, a well-known actin-binding domain. Consistent with this, actin and myosin filaments, although assembled properly, are misoriented and mislocalized in *mical* mutant muscles³⁷. Alternatively, Mical may also regulate actin cytoskeletal dynamics through the interaction of its PRD domain with Cas (Crk-associated substrate) proteins⁴⁰, which themselves regulate actin cytoskeleton organization and focal adhesion formation in non-neuronal cells⁴¹. Notably, the sole *Drosophila* homolog of Cas (DCAS), similar to Mical, is also enriched in the nervous system and genetically interacts with Mical to regulate axon guidance⁴². In response to ecdysone signaling, Mical is markedly upregulated and localizes to the dendrites of ddaC neurons. This may lead to rearrangements of dendritic actin and myofilaments that are more prone to depolymerization and disassembly in remodeling ddaC neurons. Currently, it is not known how Mical induces the severing events in dendrites but not in axons. Given the distinct local environments that axons and dendrites of ddaC neurons reside in, it is conceivable that dendritically localized Mical is activated to induce the rearrangements of dendritic actin cytoskeletons, thus inducing dendrite-severing events. Cytoskeletal rearrangements often occur as an initial sign of apoptosis⁴³. Mical is also upregulated in apoptotic dendritic arborization neurons in response to ecdysone, but loss of *mical* function has no effect in neuronal apoptosis.

Given the conservation of *sox14* and *mical* in flies and mammals, it is conceivable that regulation of *mical* by *sox14* might also be conserved and modulated by hormone responses in mammals. In response to steroid hormones, mammalian estrogen receptors, the homologs of fly EcR, are involved in mediating neurite growth and differentiation⁴⁴, as well as synapse plasticity associated with learning and memory⁴⁵. Thus, it will be of wide interest to investigate whether the EcR-Sox14-Mical pathway is evolutionarily conserved and involved in neuronal pruning and synaptic plasticity in mammals (**Supplementary Results and Discussion**).

METHODS

Methods and any associated references are available in the online version of the paper at <http://www.nature.com/natureneuroscience/>.

Note: Supplementary information is available on the Nature Neuroscience website.

ACKNOWLEDGMENTS

We thank H. Aberle, R. Barrio, Y.N. Jan, W.A. Johnson, the Bloomington Stock Center, Developmental Studies Hybridoma Bank (University of Iowa) and Vienna *Drosophila* RNAi Center for generously providing antibodies and fly stocks. We thank members of the Yu and Wang laboratories for stimulating discussions and Z.L. Ong for technical assistance. We thank W. Chia, S. Cohen, P. Rorth, S. Roy, J. Varghese and G. Feng for helpful discussions and for reading the manuscript. This work was supported by Temasek Life Sciences Laboratory (F.Y.), Duke–National

University of Singapore (MOE2008-T2-1-048 and NRF-RF2009-02 to H.W.), and grants from the US National Institutes of Health and the National Institute of Neurological Disorders and Stroke (RO1NS3165) and the Howard Hughes Medical Institute (A.L.K.). D.K. is supported by the Singapore Millennium Foundation.

AUTHOR CONTRIBUTIONS

D.K. and Y.G. conducted the majority of the experiments and data analysis on *sox14* and *mical*, respectively. Y.H. contributed to the biochemical experiments. Z.W. and A.L.K. provided reagents for *mical*. A.B. provided the pupal lethal mutant collection. B.C.L. and F.Y. cosupervised Y.G. F.Y. and H.W. conceptualized and designed the study. F.Y. supervised the project. D.K., H.W. and F.Y. wrote the manuscript.

Published online at <http://www.nature.com/natureneuroscience/>.

Reprints and permissions information is available online at <http://www.nature.com/reprintsandpermissions/>.

- Luo, L. & O'Leary, D.D. Axon retraction and degeneration in development and disease. *Annu. Rev. Neurosci.* **28**, 127–156 (2005).
- O'Leary, D.D. & Koester, S.E. Development of projection neuron types, axon pathways and patterned connections of the mammalian cortex. *Neuron* **10**, 991–1006 (1993).
- MacDonald, J.M. *et al.* The *Drosophila* cell corpse engulfment receptor Draper mediates glial clearance of severed axons. *Neuron* **50**, 869–881 (2006).
- Avery, M.A., Sheehan, A.E., Kerr, K.S., Wang, J. & Freeman, M.R. Wld S requires Nmnat1 enzymatic activity and N16-VCP interactions to suppress Wallerian degeneration. *J. Cell Biol.* **184**, 501–513 (2009).
- Hooper, E.D. *et al.* Wlds protection distinguishes axon degeneration following injury from naturally occurring developmental pruning. *Neuron* **50**, 883–895 (2006).
- Tsai, J., Grutzendler, J., Duff, K. & Gan, W.B. Fibrillar amyloid deposition leads to local synaptic abnormalities and breakage of neuronal branches. *Nat. Neurosci.* **7**, 1181–1183 (2004).
- Li, H., Li, S.H., Yu, Z.X., Shelbourne, P. & Li, X.J. Huntingtin aggregate-associated axonal degeneration is an early pathological event in Huntington's disease mice. *J. Neurosci.* **21**, 8473–8481 (2001).
- Truman, J.W. Metamorphosis of the central nervous system of *Drosophila*. *J. Neurobiol.* **21**, 1072–1084 (1990).
- Lee, T., Lee, A. & Luo, L. Development of the *Drosophila* mushroom bodies: sequential generation of three distinct types of neurons from a neuroblast. *Development* **126**, 4065–4076 (1999).
- Marin, E.C., Watts, R.J., Tanaka, N.K., Ito, K. & Luo, L. Developmentally programmed remodeling of the *Drosophila* olfactory circuit. *Development* **132**, 725–737 (2005).
- Lee, T., Marticke, S., Sung, C., Robinow, S. & Luo, L. Cell-autonomous requirement of the USP/EcR-B ecdysone receptor for mushroom body neuronal remodeling in *Drosophila*. *Neuron* **28**, 807–818 (2000).
- Watts, R.J., Hooper, E.D. & Luo, L. Axon pruning during *Drosophila* metamorphosis: evidence for local degeneration and requirement of the ubiquitin-proteasome system. *Neuron* **38**, 871–885 (2003).
- Awasaki, T. & Ito, K. Engulfment action of glial cells is required for programmed axon pruning during *Drosophila* metamorphosis. *Curr. Biol.* **14**, 668–677 (2004).
- Watts, R.J., Schuldiner, O., Perrino, J., Larsen, C. & Luo, L. Glia engulf degenerating axons during developmental axon pruning. *Curr. Biol.* **14**, 678–684 (2004).
- Awasaki, T. *et al.* Essential role of the apoptotic cell engulfment genes draper and ced-6 in programmed axon pruning during *Drosophila* metamorphosis. *Neuron* **50**, 855–867 (2006).
- Zhu, S., Chiang, A.S. & Lee, T. Development of the *Drosophila* mushroom bodies: elaboration, remodeling and spatial organization of dendrites in the calyx. *Development* **130**, 2603–2610 (2003).
- Brown, H.L., Cherkas, L., Cherkas, P. & Truman, J.W. Use of time-lapse imaging and dominant negative receptors to dissect the steroid receptor control of neuronal remodeling in *Drosophila*. *Development* **133**, 275–285 (2006).
- Schubiger, M., Wade, A.A., Carney, G.E., Truman, J.W. & Bender, M. *Drosophila* EcR-B ecdysone receptor isoforms are required for larval molting and for neuron remodeling during metamorphosis. *Development* **125**, 2053–2062 (1998).
- Williams, D.W. & Truman, J.W. Cellular mechanisms of dendrite pruning in *Drosophila*: insights from *in vivo* time-lapse of remodeling dendritic arborizing sensory neurons. *Development* **132**, 3631–3642 (2005).
- Kuo, C.T., Jan, L.Y. & Jan, Y.N. Dendrite-specific remodeling of *Drosophila* sensory neurons requires matrix metalloproteases, ubiquitin-proteasome, and ecdysone signaling. *Proc. Natl. Acad. Sci. USA* **102**, 15230–15235 (2005).
- Lee, H.H., Jan, L.Y. & Jan, Y.N. *Drosophila* IKK-related kinase Ikk2 and Katanin p60-like 1 regulate dendrite pruning of sensory neuron during metamorphosis. *Proc. Natl. Acad. Sci. USA* **106**, 6363–6368 (2009).
- Kuo, C.T., Zhu, S., Younger, S., Jan, L.Y. & Jan, Y.N. Identification of E2/E3 ubiquitinating enzymes and caspase activity regulating *Drosophila* sensory neuron dendrite pruning. *Neuron* **51**, 283–290 (2006).
- Williams, D.W., Kondo, S., Krzyzanowska, A., Hiromi, Y. & Truman, J.W. Local caspase activity directs engulfment of dendrites during pruning. *Nat. Neurosci.* **9**, 1234–1236 (2006).
- Ainsley, J.A. *et al.* Enhanced locomotion caused by loss of the *Drosophila* DEG/ENaC protein Pickpocket1. *Curr. Biol.* **13**, 1557–1563 (2003).

25. Thummel, C.S. Files on steroids—*Drosophila* metamorphosis and the mechanisms of steroid hormone action. *Trends Genet.* **12**, 306–310 (1996).
26. Zheng, X. *et al.* TGF- β signaling activates steroid hormone receptor expression during neuronal remodeling in the *Drosophila* brain. *Cell* **112**, 303–315 (2003).
27. Pauli, A. *et al.* Cell type-specific TEV protease cleavage reveals cohesin functions in *Drosophila* neurons. *Dev. Cell* **14**, 239–251 (2008).
28. Schuldiner, O. *et al.* piggyBac-based mosaic screen identifies a postmitotic function for cohesin in regulating developmental axon pruning. *Dev. Cell* **14**, 227–238 (2008).
29. Lee, C.Y. *et al.* Genome-wide analyses of steroid- and radiation-triggered programmed cell death in *Drosophila*. *Curr. Biol.* **13**, 350–357 (2003).
30. Beckstead, R.B., Lam, G. & Thummel, C.S. The genomic response to 20-hydroxyecdysone at the onset of *Drosophila* metamorphosis. *Genome Biol.* **6**, R99 (2005).
31. Li, T.R. & White, K.P. Tissue-specific gene expression and ecdysone-regulated genomic networks in *Drosophila*. *Dev. Cell* **5**, 59–72 (2003).
32. Lee, T. & Luo, L. Mosaic analysis with a repressible cell marker for studies of gene function in neuronal morphogenesis. *Neuron* **22**, 451–461 (1999).
33. Crémazy, F., Berta, P. & Girard, F. Genome-wide analysis of Sox genes in *Drosophila melanogaster*. *Mech. Dev.* **109**, 371–375 (2001).
34. Sparkes, A.C., Mumford, K.L., Patel, U.A., Newbury, S.F. & Crane-Robinson, C. Characterization of an SRY-like gene, DSox14, from *Drosophila*. *Gene* **272**, 121–129 (2001).
35. Wang, L. *et al.* A genetic screen identifies new regulators of steroid-triggered programmed cell death in *Drosophila*. *Genetics* **180**, 269–281 (2008).
36. Terman, J.R., Mao, T., Pasterkamp, R.J., Yu, H.H. & Kolodkin, A.L. MICALs, a family of conserved flavoprotein oxidoreductases, function in plexin-mediated axonal repulsion. *Cell* **109**, 887–900 (2002).
37. Beuchle, D., Schwarz, H., Langegger, M., Koch, I. & Aberle, H. *Drosophila* MICAL regulates myofilament organization and synaptic structure. *Mech. Dev.* **124**, 390–406 (2007).
38. Chittaranjan, S. *et al.* Steroid hormone control of cell death and cell survival: molecular insights using RNAi. *PLoS Genet.* **5**, e1000379 (2009).
39. Lefebvre, V., Dumitriu, B., Penzo-Mendez, A., Han, Y. & Pallavi, B. Control of cell fate and differentiation by Sry-related high-mobility-group box (Sox) transcription factors. *Int. J. Biochem. Cell Biol.* **39**, 2195–2214 (2007).
40. Suzuki, T. *et al.* MICAL, a novel CasL interacting molecule, associates with vimentin. *J. Biol. Chem.* **277**, 14933–14941 (2002).
41. Defilippi, P., Di Stefano, P. & Cabodi, S. p130Cas: a versatile scaffold in signaling networks. *Trends Cell Biol.* **16**, 257–263 (2006).
42. Huang, Z., Yazdani, U., Thompson-Peer, K.L., Kolodkin, A.L. & Terman, J.R. Crk-associated substrate (Cas) signaling protein functions with integrins to specify axon guidance during development. *Development* **134**, 2337–2347 (2007).
43. Ndozangue-Touriguine, O., Hamelin, J. & Breard, J. Cytoskeleton and apoptosis. *Biochem. Pharmacol.* **76**, 11–18 (2008).
44. Toran-Allerand, C.D., Singh, M. & Setalo, G., Jr. Novel mechanisms of estrogen action in the brain: new players in an old story. *Front. Neuroendocrinol.* **20**, 97–121 (1999).
45. McCarthy, M.M. Estradiol and the developing brain. *Physiol. Rev.* **88**, 91–124 (2008).



ONLINE METHODS

Fly strains. The following stocks were used in this study: *Mical*^{K583}, *Mical*^{K1496}, *Mical*^{l696}, *Mical*^{G56} (ref. 37), *ppk-Gal4* (ref. 24), *Df(3R)swp2^{MICAL}* (ref. 36); *UAS-Mical^{FL}*, *UAS-Mical^{N-ter}*; *Gal4²⁻²¹* (ref. 46) and *ppk-eGFP* (ref. 47). The RNAi stocks included *UAS-sox14 RNAi*, *UAS-EcR RNAi*, *UAS-usp RNAi*, *UAS-mical RNAi* and the seven RNAi lines specific to the other *Drosophila* Sox family genes; all other RNAi lines used for the initial screen were obtained from the National Institute of Genetics (Japan) and the Vienna *Drosophila* RNAi Center⁴⁸. From the Bloomington stock center, we obtained *Df(3R)BSC38*, *Df(2R)BSC136*, *Df(2R)or-BR11a*, *Df(3R)ED5438*, *Df(3R)ED5454*, *Df(3R)Exel6155*, *elav-Gal4*, *201Y-Gal4*, *UAS-mCD8GFP*, *UAS-EcR-B1-ΔC655*, *W650A TP1-9*, *Gal4¹⁰⁹⁽²⁾⁸⁰*, *FRT42D*, *FRT82B*, *tub-Gal80* and *hsFlp* flies.

Generation of *sox14* mutants. We crossed *y^l;P{y⁺[+m8]}=Mae-UAS.6.11/LA00606* flies with a fly strain carrying the Δ2-3 transposase to induce excision. About 300 lines were established on the basis of the absence of the *y⁺* marker. Nine pupal lethal lines were recovered and subjected to genomic PCR and DNA sequencing analysis. The line with a 1,964-bp deletion was named *sox14^{Δ13}* and the line with a 1,838-bp deletion was named *sox14^{Δ15}*.

Mapping of the *mical* allele. *l(3)15256* was isolated from a pupal lethal collection on the basis of its strong pruning defects. The mutation was mapped by meiotic recombination mapping and deficiency mapping. *l(3)15256* failed to complement with the deficiency *Df(3R)BSC38*. Further deficiency mapping using *Df(3R)ED5438*, *Df(3R)ED5454*, *Df(3R)Exel6155* and *Df(3R)swp2^{MICAL}* narrowed down the cytological location to 85F1-F8. The molecular lesion in the *mical* gene was confirmed by PCR from genomic DNA and sequencing.

MARCM analysis. We heat shocked 3–6-h-old embryos twice at 38 °C and aged them until they reached the late third-instar larval stage. ddaC clones were selected at the wL3 stage and imaged at the white prepupal stage according to their location and the complex stereotyped dendritic arbor morphology. The same ddaC clones were examined for dendrite-pruning defects at 18 h APF.

Plasmid constructs and antibody production. Full-length *sox14* cDNA was obtained by PCR from genomic DNA fragments and verified by DNA sequencing. It was subsequently cloned into pUAST and the resulting construct was used for microinjection and to generate transformants (Bestgene). The C-terminal region (amino acids 440–669) of Sox14 was expressed using the GST expression vector (pGEX 4T-1, Pharmacia) and the purified protein was used to immunize mice to generate antibodies to Sox14. These antibodies are specific for Sox14, as

the immunofluorescent signals seen in wild-type tissues were absent in *sox14* homozygous mutants and *sox14* RNAi neurons (**Supplementary Fig. 3** and data not shown) and the signals could be restored on the overexpression of *UAS-sox14* transgenes in a *sox14* homozygous mutant wL3 larvae (**Supplementary Fig. 3**).

Imaging and dendrite quantification. Third-instar larvae, white prepupae and prepupae until 8 h APF were directly imaged using confocal microscopy. Images of neurons were taken as maximum projections of 15–40 optical sections at ~1.5-μm intervals. Quantification of all live images was carried out by counting the number of primary and secondary dendrites in a 300- × 300-μm region of the dorsal dendritic field of the ddaC neurons, originating from the second to fifth abdominal segments.

For time-lapse imaging, time-lapse frames were assembled as maximum projections of 20–30 optical sections taken at ~1.5-μm intervals every 5 or 6 min. Movies were assembled in ImageJ with the Image5D plugin (J. Walter, University of Munich). Stills were aligned using the Stackreg plugin (P. Thévenaz, Ecole Polytechnique Fédérale de Lausanne). Images of fixed and live samples were obtained by laser confocal microscopy on a Leica SPE or Zeiss Meta510 and processed using Photoshop (Adobe Systems).

Immunohistochemistry. Primary antibodies were used at a concentration of 1:1,000 for rabbit antibody to Mical, 1:40 for mouse antibody to EcR-B1 AD4.4 (Developmental Studies Hybridoma Bank, University of Iowa), 1:50 for mouse antibody to Usp (a gift from R. Barrio, CIC BioGUNE), 1:200 for mouse antibody to Sox14, 1:1,000 for rabbit antibody to GFP and 1:100 for Cy5-conjugated goat antibody to horseradish peroxidase (Jackson Laboratories). Cy3- or fluorescein isothiocyanate (FITC)-conjugated secondary antibodies were from Jackson Laboratories. Samples were mounted in VectaShield mounting medium.

Statistical analyses. For the effect of nonfunctional and functional Mical overexpression in various mutant backgrounds, statistical significance was determined using two-tailed Student's *t* test. We considered the results to be significant when *P* < 0.001.

46. Grueber, W.B., Jan, L.Y. & Jan, Y.N. Different levels of the homeodomain protein cut regulate distinct dendrite branching patterns of *Drosophila* multidendritic neurons. *Cell* **112**, 805–818 (2003).

47. Grueber, W.B., Ye, B., Moore, A.W., Jan, L.Y. & Jan, Y.N. Dendrites of distinct classes of *Drosophila* sensory neurons show different capacities for homotypic repulsion. *Curr. Biol.* **13**, 618–626 (2003).

48. Dietzl, G. *et al.* A genome-wide transgenic RNAi library for conditional gene inactivation in *Drosophila*. *Nature* **448**, 151–156 (2007).